

X. LIU*, D.R. QUEEN**, T.H. METCALF*, J.E. KAREL***, F. HELLMAN****,****

AMORPHOUS DIELECTRIC THIN FILMS WITH EXTREMELY LOW MECHANICAL LOSS

AMORFICZNE CIENKIE WARSTWY DIELEKTRYCZNE Z BARDZO MAŁĄ WIELKOŚCIĄ STRAT MECHANICZNYCH

The ubiquitous low-energy excitations are one of the universal phenomena of amorphous solids. These excitations dominate the acoustic, dielectric, and thermal properties of structurally disordered solids. One exception has been a type of hydrogenated amorphous silicon (α -Si:H) with 1 at.% H. Using low temperature elastic and thermal measurements of electron-beam evaporated amorphous silicon (α -Si), we show that TLS can be eliminated in this system as the films become denser and more structurally ordered under certain deposition conditions. Our results demonstrate that TLS are not intrinsic to the glassy state but instead reside in low density regions of the amorphous network. This work obviates the role hydrogen was previously thought to play in removing TLS in α -Si:H and favors an ideal four-fold covalently bonded amorphous structure as the cause for the disappearance of TLS. Our result supports the notion that α -Si can be made a “perfect glass” with “crystal-like” properties, thus offering an encouraging opportunity to use it as a simple crystal dielectric alternative in applications, such as in modern quantum devices where TLS are the source of dissipation, decoherence and $1/f$ noise.

Keywords: Internal friction, amorphous silicon, elastic modulus, speed of sound, tunneling systems

Wszechobecne niskoenergetyczne wzbudzenia są jednym z powszechnych zjawisk w amorficznych ciałach stałych. Wzbudzenia te dominują akustyczne, dielektryczne i termiczne właściwości strukturalnie nieuporządkowanych ciał stałych. Wyjątkiem jest rodzaj uwodornionego amorficznego krzemu (α -Si:H) o zawartości 1 at.% H. Na podstawie niskotemperaturowych badań własności sprężystych i termicznych krzemu amorficznego (α -Si) naparowanego wiązką elektronów wykazaliśmy, że w pewnych warunkach osadzania można wyeliminować TLS w tym układzie tak, że warstwy stają się gęstsze i strukturalnie bardziej uporządkowane. Uzyskane przez nas wyniki wskazują, że TLS nie są nieodłączną cechą stanu szklistego, ale lokują się w regionach o niskim zagęszczeniu sieci amorficznej. Praca niniejsza wyjaśnia, że wodór nie pełni roli w usuwaniu TLS w α -Si:H, jak dotąd sądzono, i wskazuje na idealną czterokrotnie kowalencyjnie związaną amorficzną strukturę jako przyczynę znikania TLS. Nasz wynik potwierdza koncepcję, że z α -Si można wytworzyć ”doskonałe szkło” o ”podobnych do krystalicznych” właściwościach, oferując w ten sposób zachęcającą możliwość wykorzystania go alternatywnie jako prosty krystaliczny dielektryk w takich aplikacjach jak w nowoczesne urządzenia kwantowe, gdzie TLS są źródłem dyssypacji dekoherencji i szumu $1/f$.

1. Introduction

Amorphous solids exhibit many universal phenomena that are absent in crystalline solids. One such example is the low energy excitations [1], where, at low temperatures, only the propagating phonons that give rise to the T^3 Debye specific heat are expected. While in crystals defects usually have characteristic energies, the low energy excitations have a broad and almost energy independent distribution. They are the source of anomalous thermal, elastic and dielectric properties of amorphous solids [2], such as: a linear T dependent specific heat, T^2 thermal conductivity below 1 K, and an almost T independent plateau in internal friction at a few degrees K. These properties are thought to be universal due to the quantitative similarities for a wide variety of amorphous solids. The model

of two-level tunneling systems (TLS) provides a phenomenological description for the low energy excitations by assuming that a small number of atoms or groups of atoms with energetically similar configurations can tunnel between the minima of neighboring double-well potentials in amorphous energy landscape [3,4]. But the TLS model does not provide a microscopic description of the tunneling entities and the cause of universality. The nature of the low energy excitations of amorphous solids remains one of the unsolved mysteries in condensed matter physics.

Amorphous Si (α -Si) has been a model system for covalent amorphous solids [5]. In fact, the first amorphous solids without TLS were found 15 years ago in a type of hydrogenated amorphous silicon (α -Si:H) thin films containing 1 at.% H prepared by hot-wire chemical-vapor deposition [6].

* NAVAL RESEARCH LABORATORY, CODE 7130, WASHINGTON, DC 20375, USA

** NRC POSTDOCTORAL ASSOCIATE, CODE 7130, WASHINGTON, DC 20375, USA

*** DEPARTMENT OF MATERIALS SCIENCE AND ENGINEERING, UNIVERSITY OF CALIFORNIA, BERKELEY, BERKELEY, CALIFORNIA 94720, USA

**** DEPARTMENT OF PHYSICS, UNIVERSITY OF CALIFORNIA, BERKELEY, BERKELEY, CALIFORNIA 94720, USA

Subsequent research was interpreted as showing that meticulous incorporation of a small amount of H eliminated TLS by passivating dangling bonds [7]. Now, we show that *a*-Si thin films prepared by electron-beam (*e*-beam) evaporation without H but at a growth temperature (T_{sub}) of 400°C, comparable to that of *a*-Si:H with 1 at.% H, also contain few TLS, despite still containing significant numbers of dangling bonds. This result supports Phillips original suggestion that TLS are unlikely to form in overconstrained amorphous systems [4] and suggests that the structure of *a*-Si is heterogeneous with TLS occurring in the low density regions [8]. This finding gives new insight into the microscopic origin of TLS. It also comes at a time when TLS in dielectric amorphous thin films have become a bottleneck in an array of cutting edge technologies as they cause both elastic and dielectric losses. TLS limit the elastic quality factor in both nanomechanical and quantum resonators [9], and are the dominant decoherence source in superconducting quantum bits [10].

2. Experimental and results

The *a*-Si thin films studied in this work were grown by *e*-beam evaporation at $T_{sub} = 45, 200, 300, 350,$ and 400°C. All films were approximately 300 nm thick, measured by an Alpha-Step IQ profilometer. Companion *a*-Si films deposited at the same time or in identical conditions were examined by Raman spectroscopy, electron and X-ray diffraction, and transmission electron microscopy [8]. Mass density was measured with Rutherford backscattering: $\rho = 2.02, 2.14, 2.18 \text{ g/cm}^3$ for films with $T_{sub} = 45, 200,$ and 350°C, respectively, and $\rho = 2.17$ and 2.22 g/cm^3 for the two films with $T_{sub} = 400^\circ\text{C}$. All films are found to be fully amorphous and exhibit increased structural order and mass density with the increase of T_{sub} . We measured the complex elastic properties, including the real (shear modulus, G_{film} , and relative change of speed of sound, $\frac{\Delta v}{v_0}$) and the imaginary (internal friction, Q^{-1}) parts, of *e*-beam *a*-Si films from 0.4 K to room temperature by using the double-paddle oscillator (DPO) technique [11,12]. Due to its excellent vibration isolation, the low background Q^{-1} ($\sim 1 \times 10^{-8}$) of the torsional vibration mode ($\sim 5500 \text{ kHz}$) used in this work ensures high sensitivity of the technique

to extract elastic properties of thin films. The finite-element simulated mode shape of the DPO is illustrated in the inset of Fig. 1(a). The DPOs were coupled to two electrodes behind the wings. They were driven and detected electrostatically. The resonance was phase-locked in a self-exciting loop, from which the resonance frequency is determined by a high resolution frequency counter. The internal friction Q^{-1} was calculated from the amplitude-over-time free ring-down measurement, regarded as the classical “wave-height” methods [13].

Addition of a film on the neck area, see the insert of Fig. 1(a), leads to a measurable shift of a DPO’s resonance frequency, from f_{sub} to f_{osc} , and the internal friction, from Q_{sub}^{-1} to Q_{osc}^{-1} . From the shift, the shear modulus, G_{film} , the internal friction, Q_{film}^{-1} , and the relative change of speed of sound, $\left(\frac{\Delta v}{v_0}\right)_{film} = \frac{v_{film} - v_{film}(T_0)}{v_{film}(T_0)}$ of the film can be calculated through,

$$\frac{f_{osc} - f_{sub}}{f_{sub}} = \frac{3G_{film}t_{film}}{2G_{sub}t_{sub}}, \quad (1)$$

$$Q_{film}^{-1} = \frac{G_{sub}t_{sub}}{3G_{film}t_{film}} (Q_{osc}^{-1} - Q_{sub}^{-1}) + Q_{osc}^{-1}, \quad (2)$$

$$\left(\frac{\Delta v}{v_0}\right)_{film} = \frac{G_{sub}t_{sub}}{3G_{film}t_{film}} \left[\left(\frac{\Delta f}{f_0}\right)_{osc} - \left(\frac{\Delta f}{f_0}\right)_{sub} \right] + \left(\frac{\Delta v}{v_0}\right)_{sub}, \quad (3)$$

where $t, G,$ and $\frac{\Delta f}{f_0} = \frac{f(T) - f(T_0)}{f(T_0)}$ are thicknesses, shear moduli, and relative change of resonant frequency, respectively of the oscillators, the substrates, and the films. T_0 is a reference temperature, usually taken as the lowest temperature point of the experiment. The shear modulus of silicon along the neck of DPOs ($\langle 110 \rangle$) is $G_{sub} = 62 \text{ GPa}$, and $t_{sub} = 300 \mu\text{m}$.

The representative temperature dependent resonant frequency of two DPOs before and after *e*-beam *a*-Si evaporation at $T_{sub} = 45$ and 400°C is shown in Figs. 1(a) and (b), respectively. The frequency shift is proportional to G_{film} . We calculate the average G_{film} by subtracting resonant frequency with films and its background at low temperatures (below 30 K) where Q_{osc}^{-1} the lowest and f is relatively temperature independent. These low temperature G_{film} values are about 5% higher than those measured at room temperature. The low temperature data for all the films studied in this work are shown in Fig. 1(c). G_{film} increases with T_{sub} , but even for the

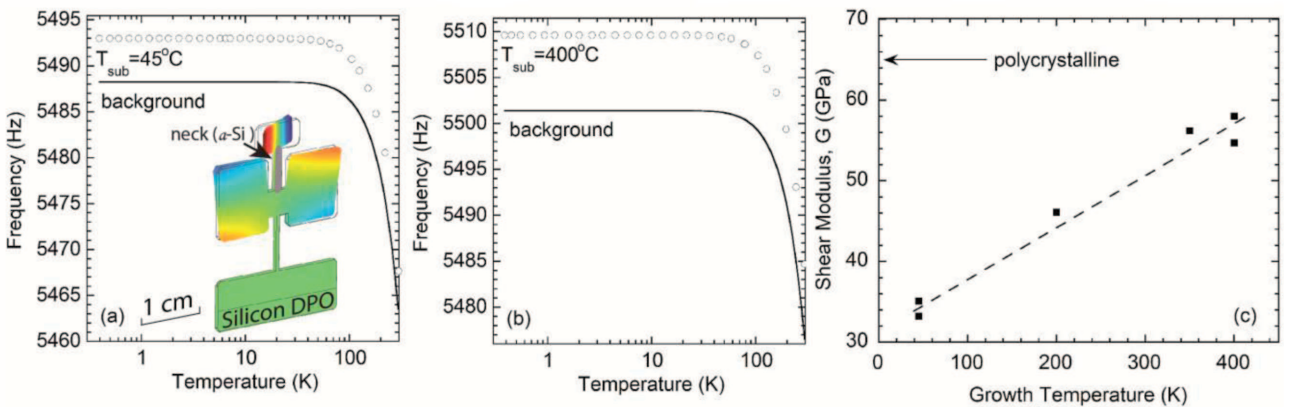


Fig. 1. The resonant frequency of DPOs before and after *e*-beam deposition of *a*-Si at 45°C (a) and 400°C (b). The inset in (a) shows the finite-element simulated torsional mode used in this work. Films are deposited in the gray-colored neck area where most of the shear strain is concentrated. (c) G_{film} vs. T_{sub} . The dashed line is a guide to the eye. The G of polycrystalline silicon (65 GPa) is indicated by an arrow

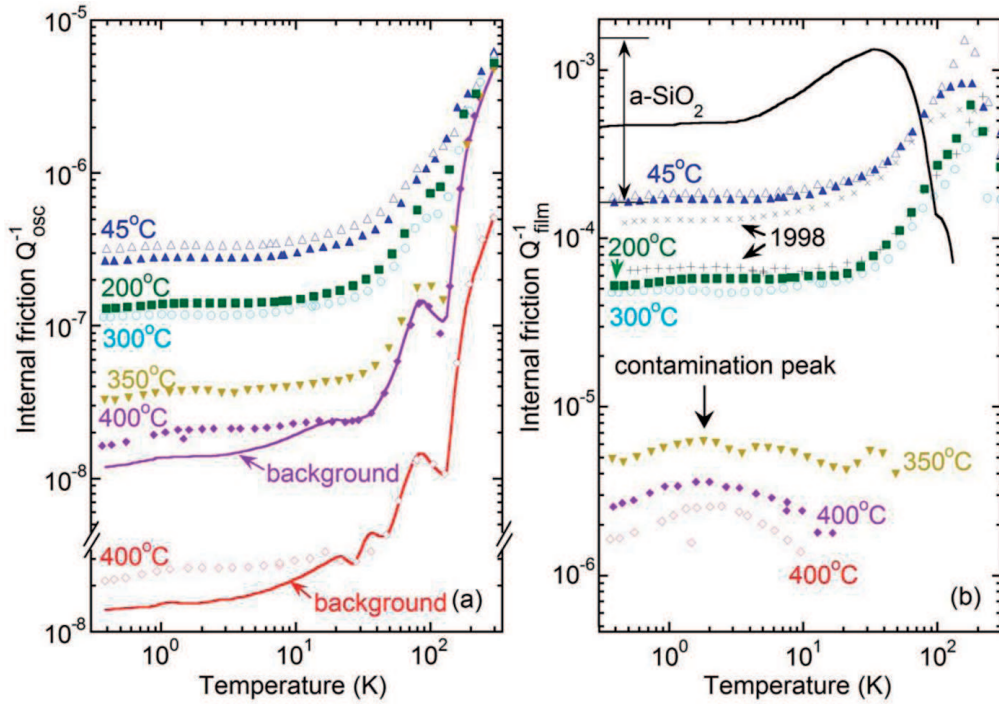


Fig. 2. (a) Q_{osc}^{-1} of DPOs carrying e-beam a-Si films. The two 400°C films with their respective backgrounds (solid lines) are shown in a y-axis shifted view. (b) Q_{film}^{-1} of e-beam a-Si films and a 107 nm thick dry thermal oxide for comparison. The data labelled “1998” are from an earlier study [7] deposited at room temperature (x) and annealed at 350°C for 5 hours (+). The label “contamination peak” denotes that a large portion of Q_{film}^{-1} for the 350 and 400°C films includes contamination induced loss in the DPO substrate, not related to the a-Si films. The double arrow denotes the “glassy range” explained in the text

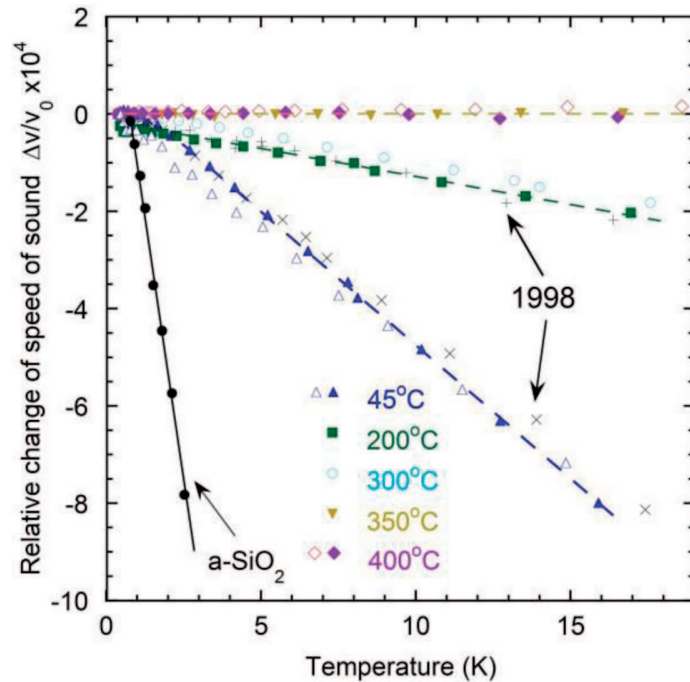


Fig. 3. $\frac{\Delta v}{v_0}$ of the e-beam a-Si films, and a 107 nm thick dry thermal oxide film for comparison. The data labelled “1998” are from an earlier study [7] deposited at room temperature (x) and annealed at 350°C for 5 hours (+). The straight lines indicate the linear temperature dependence explained in the text

largest G_{film} (at $T_{sub} = 400^\circ\text{C}$), it is still below that of polycrystalline silicon [14]. The error bars on G_{film} are comparable to the variations seen in different films prepared at the same growth temperatures (e.g. at 45 and 400°C).

The internal friction of DPOs, Q_{osc}^{-1} , carrying e-beam a-Si films deposited at different temperatures are shown in Fig. 2(a). To calculate the internal friction of the films, Q_{film}^{-1} , the background internal friction of the DPOs, Q_{sub}^{-1} , was sep-

arately measured. We only show Q_{osc}^{-1} with their respective Q_{sub}^{-1} for the two $T_{\text{sub}} = 400^\circ\text{C}$ films in Fig. 2(a) with the y-axis shifted for clarity. Thermoelastic loss dominates Q_{sub}^{-1} above 50 K [15] while clamp loss is thought to dominate below 50 K. The internal friction data of the films Q_{film}^{-1} are shown in Fig. 2(b).

The relaxational scattering of elastic waves by TLS contributes to the temperature independent plateau in internal friction, Q_0^{-1} , which is described by the tunneling strength C in the TLS model, as [16]

$$Q_0^{-1} = \frac{\pi}{2}C, \quad (4)$$

where C is defined as

$$C = \frac{\bar{P}\gamma^2}{\rho\nu^2} \quad (5)$$

and \bar{P} is the spectral density of the tunneling states, γ the energy with which they are coupled to phonons, ρ the mass density, and ν the speed of sound. With the exception of *a*-Si:H [6], Q_0^{-1} varies within a range of about one order of magnitude for most amorphous solids, often called the “glassy range”. For comparison with prototypical amorphous solids, Fig. 2(b) shows the Q_{film}^{-1} of a 107 nm thick dry thermal oxide (*a*-SiO₂) film grown directly on a DPO at 1100°C. The double arrow shows the glassy range. The universal magnitude Q_0^{-1} of is surprising given the individual parameters that constitute C , like mass density ρ or elastic constants $\rho\nu^2$, may vary by many orders of magnitude [16]. Thus, a measurement Q_0^{-1} of directly reveals the universality of the low-energy excitations as well as the spectral density of TLS.

The Q_{film}^{-1} of *e*-beam *a*-Si films decreases with increasing T_{sub} . The Q_{film}^{-1} data of both 45°C films agree with an earlier result labelled as “1998” in Fig. 2(b) [7] as they sit right at the bottom of the glassy range. However, the of Q_{film}^{-1} 200°C is smaller than that of the earlier result of an *e*-beam *a*-Si film annealed at 350°C for 5 hours after deposition at room temperature, also labelled as “1998” in Fig. 2(b) [7], indicating that elevated growth temperature, or surface energetics, is more effective than annealing to remove TLS (a similar effect was seen in work on *a*-Tb-Fe [17]). As T_{sub} continues to rise, Q_{film}^{-1} drops rapidly, reaching an almost undetectable level above 10 K for both 400°C. Note that the sample with higher ρ has lower Q_{film}^{-1} .

It is clear from both Figs. 2(a) and (b) that the Q_{film}^{-1} of 350 and 400°C below 10 K is not only very low but is also not flat in temperature as one would expect from the TLS contribution. This behavior is reminiscent of the annealing related contamination effect on DPOs that we observed in the study of *a*-Si:H films deposited at approximately the same temperature [6]. It is known that DPOs are extremely sensitive to contamination by surface dopants when heated above 300°C, causing a broad contamination peak in internal friction labelled in Fig. 2(b) that is not in the films [18]. The important observation is that the internal friction plateau characteristic of TLS diminishes as T_{sub} increases. Since Q_{osc}^{-1} for both 400°C films is within the experimental uncertainty of their respective background above 20 K, we presume a detection limit of $\Delta Q_{\text{min}}^{-1} = 5 \times 10^{-10}$ and calculate an upper bound of $Q_{\text{film}}^{-1} \leq 2 \times 10^{-7}$. This is comparable to that of *a*-Si:H with 1 at.% H [6], and is three orders of magnitude smaller than the glassy range shown in Fig. 2(b).

Another way to confirm that the *e*-beam *a*-Si films lose their glassy behavior with the increase of T_{sub} is to measure the real part of the elastic constant, which yields the variation of the speed of sound with temperature calculated from the resonance frequencies. The characteristic features of $\frac{\Delta\nu}{\nu_0}$ by resonant and relaxational scattering by TLS occur at lower temperatures than we have used in this work. However, $\frac{\Delta\nu}{\nu_0}$ is known to vary linearly with temperature in amorphous solids from a few K up to a few tens of K [19]: $\frac{\Delta\nu}{\nu_0} = -\beta(T - T_0)$, where β is proportional to C and Q_0^{-1} for all amorphous solids studied [20]. This dependence at higher T is understood as the thermally activated relaxation rate of the TLS dominating the quantum tunneling rate [21]. The results of the change in speed of sound for the same films shown in Fig. 2, including the two *e*-beam *a*-Si films from an earlier study [7], are shown in Fig. 3. Similar to Q_{film}^{-1} shown in Fig. 2(b), β diminishes to an undetectable level with the increase of T_{sub} . The large β of the thermal oxide film is consistent with its high Q_{film}^{-1} .

3. Discussion

Since elastic measurements always probe \bar{P} and γ^2 together (see Eqs. (4),(5)), it is theoretically possible that the growth temperature effect that we see comes from a diminishing phonon coupling of TLS. This is however ruled out by the results of low temperature specific heat measurements on similarly prepared *e*-beam *a*-Si films [8]. Specific heat measurements show that the density of TLS reduces by a factor of 20 for films with comparable thickness as T_{sub} increases from 45°C to 400°C. These results together convincingly confirm a significant reduction of the density of TLS in *a*-Si. At the same time, the proportionality of the density of TLS from specific heat and the coupling strength from internal friction rule out anomalous excitations other than TLS as the source of non-Debye specific heat at low temperatures.

In this work, we show that H is not a necessary ingredient for the absence of TLS in *e*-beam *a*-Si. As ESR measurements show that the dangling bond density is $\sim 10^{18} \text{ cm}^{-3}$ in the 400°C *e*-beam *a*-Si [8] vs. $\sim 10^{16} \text{ cm}^{-3}$ in *a*-Si:H with 1 at.% H despite similarly low TLS [6]. As H content is mostly controlled by T_{sub} , we suggest the *a*-Si:H results should be re-interpreted as a T_{sub} dependence due to surface energetics. It is an unlikely coincidence that the disappearance of TLS occurs at comparable T_{sub} for both for different reasons. In fact, ruling out H as a necessary contributor points to the structure of *a*-Si as the cause for the disappearance of TLS, namely, the formation of a dense tetrahedrally bonded network. This supports the suggestion made by Phillips 40 years ago, in which he speculated that TLS may originate from an “open structure” with “low coordination” [4]. He argued that if every atom is linked to more than two neighbors (like in *a*-Si and *a*-Ge), the structure is rigid and double-well potentials are unlikely. Previous work has shown empirically that adding H reduced the dangling bond density and the TLS. In this work, we demonstrate that these effects can and should be considered separately. Our results emphasize the importance of structural rigidity.

The strong mass density dependence observed here and in the specific heat measurements [8] also points out the struc-

tural heterogeneity may be equally important. As amorphous solids are generally less dense than their crystalline counterparts, it may be that TLS originate from the low density regions of an amorphous network. This is reminiscent of the free volume model where sufficient volume is required to form a TLS [22]. TLS may form as a result of free volume available on the atomic scale for atoms to tunnel. Therefore, we may significantly reduce TLS density in any amorphous solid, including those with low atomic coordination, by removing low density regions that cause tunneling. More work is needed to distinguish the roles played by rigidity and heterogeneity in amorphous solids and to reveal the microscopic origin of the universal low energy excitations.

4. Conclusions

To conclude, this work demonstrates that TLS can be removed from hydrogen-free *a*-Si by proper optimization of deposition conditions, thus revealing a clear dependence of TLS on macroscopic parameters and microstructure. This opens up an avenue to further elucidate the microscopic origin of TLS as well as the other universal phenomena of amorphous solids. Our result supports the notion that *a*-Si can be made a “perfect glass” [23] with “crystal-like” properties, thus offering an encouraging opportunity to use it as an easy to prepare alternative to crystalline materials in applications, such as in modern quantum devices where TLS are the source of dissipation, decoherence and $1/f$ noise.

Acknowledgements

This work was supported by the Office of Naval Research and NSF DMR-0907724. Film growth was supported by the U.S. Department of Energy DE-AC02-05CH11231.

REFERENCES

- [1] R.C. Zeller, R.O. Pohl, Thermal conductivity and specific heat of noncrystalline solids, *Phys. Rev. B* **4**, 2029-2041 (1971).
- [2] W.A. Phillips, *Amorphous solids – Low Temperature Properties*, Springer, Berlin, 1981.
- [3] P.W. Anderson, B.I. Halperin, C.M. Varma, Anomalous low-temperature thermal properties of glasses and spin glasses, *Philos. Mag.* **25**, 1-9 (1972).
- [4] W.A. Phillips, Tunneling states in amorphous solids, *J. Low Temp. Phys.* **7**, 351-360 (1972).
- [5] M.M.J. Treacy, K.B. Borisenko, The local structure of amorphous silicon, *Science* **335**, 950-953 (2012).
- [6] X. Liu, B.E. White Jr., R.O. Pohl, E. Iwanizcko, K.M. Jones, A.H. Mahan, B.N. Nelson, R.S. Crandall, S. Veprek, Amorphous solid without low energy excitations, *Phys. Rev. Lett.* **78**, 4418-4421 (1997).
- [7] X. Liu, R.O. Pohl, Low-energy excitations in amorphous films of silicon and germanium, *Phys. Rev. B* **58**, 9067-9081 (1998).
- [8] D.R. Queen, X. Liu, J. Karel, T.H. Metcalf, F. Hellman, Excess specific heat in evaporated amorphous silicon, *Phys. Rev. Lett.* **110**, 135901 (2013).
- [9] Y.-S. Park, H. Wang, Resolved-sideband and cryogenic cooling of an optomechanical resonator, *Nat. Phys.* **5**, 489-493 (2009).
- [10] J.M. Martinis, K.B. Cooper, R. McDermott, M. Steffen, M. Ansmann, K.D. Osborn, K. Cicak, S. Oh, D.P. Pappas, R.W. Simmonds, C.C. Yu, Decoherence in josephson qubits from dielectric loss, *Phys. Rev. Lett.* **95**, 210503 (2005).
- [11] B.E. White Jr., R.O. Pohl, Elastic properties of thin films, in S.P. Baker, C.A. Ross, P.H. Townsend, C.A. Volkert, and P. Borgeisen (Eds.), *Thin films: stresses and mechanical properties V, MRS Symposia Proceedings Vol. 356*, Materials Research Society, Pittsburgh, 567-572 (1995).
- [12] C.L. Spiel, R. O. Pohl, A.T. Zehnder, Normal modes of a Si(100) double-paddle oscillator, *Rev. Sci. Instrum.* **72**, 1482-1491 (2001).
- [13] L.B. Magalas, Determination of the logarithmic decrement in mechanical spectroscopy, *Solid State Phenomena* **115**, 7-14 (2006).
- [14] M. Hopcroft, W. Nix, T. Kenny, What is the Young’s modulus of silicon? *J. Microelectromech. Sci.* **19**, 229-238 (2010).
- [15] B.H. Houston, D.M. Photiadis, M.H. Marcus, J.A. Bucaro, X. Liu, J.F. Vignola, Thermoelastic loss in microscale oscillators, *Appl. Phys. Lett.* **80**, 1300-1302 (2002).
- [16] R.O. Pohl, X. Liu, E. Thompson, Low-temperature thermal conductivity and acoustic attenuation in amorphous solids, *Rev. Mod. Phys.* **74**, 991-1013 (2002).
- [17] F. Hellman, Surface-induced ordering: A model for vapor-deposition growth of amorphous materials, *Appl. Phys. Lett.* **64**, 1947-1949 (1994).
- [18] X. Liu, R.O. Pohl, S. Asher, R.S. Crandall, Contamination of silicon during ion-implantation and annealing, *J. Non-Cryst. Solids* **227**, 407-410 (1998).
- [19] G. Bellessa, Frequency and temperature dependence of the sound velocity in amorphous materials at low temperatures, *Phys. Rev. Lett.* **40**, 1456-1459 (1978).
- [20] B.E. White Jr., R.O. Pohl, Elastic properties of amorphous solids below 100 K, *Z. Phys. B* **100**, 401-408 (1997).
- [21] D. Tielbörger, R. Merz, R. Ehrenfels, S. Hunklinger, Thermally activated relaxation processes in vitreous silica: An investigation by Brillouin scattering at high pressures, *Phys. Rev. B* **45**, 2750-2760 (1992).
- [22] M.H. Cohen, G.S. Grest, Origin of low-temperature tunneling states in glasses, *Phys. Rev. Lett.* **45**, 1271-1274 (1980).
- [23] C.A. Angell, Ten questions on glassformers, and a real space ‘excitations’ model with some answers on fragility and phase transitions, *J. Phys. Condens. Matter* **12**, 6463-6475 (2000).